Catalysis Today 232 (2014) 119–126

Contents lists available at ScienceDirect

Catalysis Today

journal homepage: www.elsevier.com/locate/cattod

# Upgrading of bio-oil derived from biomass constituents over hierarchical unilamellar mesoporous MFI nanosheets

Hyung Won Lee[a], Sung Hoon Park[b], Jong-Ki Jeon[c], Ryong Ryoo[d,e], Wookdong Kim[d,e], Dong Jin Suh[f], Young-Kwon Park[a,g,*]

[a] Graduate School of Energy and Environmental System Engineering, University of Seoul, Seoul 130-743, Republic of Korea
[b] Department of Environmental Engineering, Sunchon National University, Suncheon 540-950, Republic of Korea
[c] Department of Chemical Engineering, Kongju National University, Cheonan 330-717, Republic of Korea
[d] Center for Nanomaterials and Chemical Reactions, Institute for Basic Science (IBS), Daejeon 305-701, Republic of Korea
[e] Department of Chemistry, KAIST, Daejeon 305-701, Republic of Korea
[f] Clean Energy Research Center, Korea Institute of Science and Technology, Seoul 136-791, Republic of Korea
[g] School of Environmental Engineering, University of Seoul, Seoul 130-743, Republic of Korea

ARTICLE INFO

*Article history:*
Received 17 July 2013
Received in revised form
23 November 2013
Accepted 16 December 2013
Available online 7 January 2014

*Keywords:*
Cellulose
Hemicellulose
Lignin
Pyrolysis
Unilamellar mesoporous MFI nanosheets

ABSTRACT

Unilamellar mesoporous MFI nanosheets (UMNs) were, for the first time, applied to the catalytic pyrolysis of the constituents of lignocellulosic biomass: cellulose, hemicellulose and lignin. A representative mesoporous catalyst, Al-SBA-15, was also applied to the same process for the purpose of comparison. The catalysts were characterized by $N_2$ adsorption–desorption, X-ray diffraction, temperature programmed desorption of ammonia, and transmission electron microscopy. The synthesized UMN catalyst was composed of a random assembly of zeolite nanosheets with a thickness of 2.5 nm. UMN was shown to have strong Brønsted acid sites, whereas Al-SBA-15 had weak acid sites. Catalytic pyrolysis experiments were carried out using Py-GC/MS. The product distribution was analyzed in order to evaluate catalytic activity. Acidity had a considerable influence on catalytic activity; UMN, with a higher acidity than Al-SBA-15, exhibited higher activities for cracking and deoxygenation, producing bio-oil with a lower oxygen content and with a better overall quality. Levoglucosan, which was the main product of the non-catalytic pyrolysis of cellulose, was converted to aromatics and furans on the acid sites of the catalysts. Ketones, alcohols and cyclo-compounds, the main products of the non-catalytic pyrolysis of xylan, were also converted to aromatics and furans by catalytic upgrading. The main products of the non-catalytic pyrolysis of lignin were phenolics, which were converted to aromatics and lighter phenolics (alkyl phenolics and methoxy phenolics) in the presence of catalysts. Increasing the catalyst dose improved the quality of the product oil even further.



## 1. Introduction

The replacement of fossil fuels with renewable energies, such as bio-energy, wind energy, and solar energy, largely in order to reduce the emission of gasses related to global warming, is a worldwide trend. For instance, power stations in South Korea are legally obliged to produce a certain fraction of their total energy production from renewable energy sources. To fulfill this obligation, many power stations and local heating corporations produce electricity by combusting combinations of conventional fossil fuels and bio-fuels. Bio-fuels that are widely used include bio-diesel produced from the transesterification of vegetable oils, bio-oil and syngas produced from thermochemical conversion processes, and bio-ethanol produced from biological fermentation [1–5].

Pyrolysis is a thermochemical conversion process through which biomass is decomposed to liquid (bio-oil), solid (bio-char), and gas products by heating under oxygen-free conditions. Normally, pyrolysis is aimed at maximizing the yield of bio-oil, which can be used as a fuel for boilers, or as a feedstock for the production of phenolic resin and biochemicals with high value-added [6–8].

The production of bio-fuels from cultivated plants has brought about a sharp rise of grain prices, which has ultimately had a direct impact on the global food shortage. Consequently, this has turned the attention of many researchers to the production of bio-fuels from non-food biomass materials. Lignocellulosic biomass is receiving particular attention due to its vast reserves throughout the earth. A number of different lignocellulosic biomass materials, such as woody biomass and herbaceous biomass, have been

* Corresponding author at: School of Environmental Engineering, University of Seoul, Seoul 130-743, Republic of Korea. Tel.: +82 2 6490 5870; fax: +82 2 6490 2859.
*E-mail address:* catalica@uos.ac.kr (Y.-K. Park).

0920-5861/$ – see front matter © 2013 Elsevier B.V. All rights reserved.
http://dx.doi.org/10.1016/j.cattod.2013.12.015

used in the pyrolysis processes using different types of reactors, such as fluidized bed reactors, fixed bed reactors, and Py-GC/MS [6–11]. However, bio-oil produced from pyrolysis processes has several shortcomings, such as high oxygen content and low pH. One promising method to improve the quality of bio-oil is catalytic pyrolysis. During catalytic pyrolysis processes, the quality of bio-oil is improved by deoxygenation reactions which occur on the surface of acidic catalysts, such as zeolite. A number of different solid acid catalysts have previously been used, including microporous zeolite materials such as HZSM-5, HY and Hβ; mesoporous materials such as Al-MCM-41, Al-MCM-48 and Al-SBA-15, as well as hierarchical zeolite materials such as meso-MFI and MMZ [10–16]. All these catalysts could improve the quality of bio-oil compared to non-catalytic pyrolysis. Detailed reviews on the catalytic pyrolysis of biomass have recently been published [14,15].

While the catalytic pyrolysis of lignocellulosic biomass materials have been studied extensively, investigations of the catalytic pyrolysis of their constituents, i.e., cellulose, hemicellulose and lignin, has been relatively limited. Moreover, in most studies of the catalytic pyrolysis of biomass constituents, microporous zeolites, such as HZSM-5 and HY, were used [17–26]. Meanwhile, a few papers have reported the application of mesoporous catalysts, such as Al-MCM-41 and Al-SBA-15, to the catalytic pyrolysis of the constituents of lignocellulosic biomass [27–31].

Also, hierarchical mesoporous MFI zeolite has been reported to exhibit high catalytic activity for the pyrolysis of biomass by our previous publications [10,12,13] as well as by other researchers [32]. However, the catalytic pyrolysis of biomass constituents over hierarchical mesoporous MFI has seldom been reported. Hierarchical mesoporous MFI is expected to have a high activity for the catalytic pyrolysis of biomass constituents because its acidic property is excellent. In particular, Ryoo et al. recently reported the synthesis of a unilamellar MFI nanosheet with intersheet mesopores [33]. The thickness of the unilamellar mesoporous MFI nanosheet (UMN) was ca. 2 nm, and it was determined to have high thermal and hydrothermal stability as well as a comparable amount of strong acid sites to that of a conventional MFI catalyst [33]. It was reported that the synthesized UMN had much higher activity and stability than the conventional MFI catalyst for various catalytic reactions, including the catalytic pyrolysis of plastics and the conversion of methanol to gasoline conversion. Besides, UMN has shown a high activity for the Bechmann rearrangement of cyclohexanone oxime to ε-caprolactam [34] as well as for the conversion of bulky molecules [35]. However, UMN has not previously been applied to the catalytic upgrading of bio-oil consisting of bulky molecules. Therefore, investigations of the catalytic pyrolysis of biomass constituents over UMN are required in order to understand the relation between the catalyst characteristics and bio-oil upgrading effect, as well as for estimations of the potential of UMN for the catalytic pyrolysis of various biomass materials.

In this study, UMN was applied, for the first time, to the catalytic pyrolysis of biomass constituents. Py-GC/MS was used for the real-time analysis of the pyrolysis products. The catalytic activity of UMN was compared to that of a representative mesoporous material, Al-SBA-15.

## 2. Experimental

### 2.1. Biomass sample

Commercial cellulose (product number: 310697) and xylan (model compound of hemicellulose, product number: x4252) were purchased from Sigma–Aldrich. Lignin (dealkaline, product number: L0045) was purchased from Tokyo chemical industry. Proximate and ultimate analyses of each biomass constituent were conducted based on a previously reported method [9]. Thermogravimetric analysis (TGA) was performed following a previously reported method [9].

### 2.2. Synthesis of the catalyst

UMN was synthesized using a previously reported procedure [36], using a surfactant with a molecular formula of $[C_{16}H_{33}–N^+(CH_3)_2–C_6H_{12}–N^+(CH_3)_2–C_6H_{13}](Br^-)_2$ as a structure-directing agent (SDA). In a typical synthesis, 6.03 g of SDA was dissolved in 57.04 g of diluted sodium silicate solution (Si/Na = 1.75, 13.2 wt% $SiO_2$). A solution containing 0.24 g of sodium aluminate (53 wt% $Al_2O_3$ and 42.5 wt% $Na_2O$, Sigma–Aldrich) and 20.00 g of $H_2O$ was added dropwise under vigorous stirring. Subsequently, the mixture was further stirred for 6 h in an oven which was maintained at 60 °C. 26.26 g of diluted sulfuric acid (11.2 wt% $H_2SO_4$) was added to this mixture at once. The resultant mixture was immediately shaken by hand for 5 min and the mixture was then stirred for 6 h in an oven at 60 °C. The final molar composition of the synthesized gel was 100 $SiO_2$:1 $Al_2O_3$:7.5 SDA:30 $Na_2O$:24 $H_2SO_4$:4000 $H_2O$. The gel was heated in a Teflon-lined stainless steel autoclave at 150 °C with tumbling. After hydrothermal treatment for 5 days, the zeolite product was filtered and washed with distilled water. The product was then dried for 12 h at 100 °C and was subsequently calcined under an air flow at 550 °C to remove any remaining surfactant. The calcined zeolite was ion-exchanged into the $NH_4^+$ form by repeating the ion-exchange procedure three times with 1 M $NH_4NO_3$. The $NH_4^+$ of zeolite was converted to $H^+$ through calcination at 550 °C. Al-SBA-15 was synthesized using a method which was suggested by a previous study [37].

### 2.3. Characterization of catalysts

X-ray diffraction (XRD) patterns were collected between $2\theta$ angles of 5 and 35° using a Rigaku Multiflex diffractometer and Cu Kα radiation (30 kV, 40 mA). Nitrogen adsorption isotherms were obtained at the liquid nitrogen temperature (−196 °C) using a Micromeritics TriStar-II volumetric adsorption analyzer. Prior to each measurement, the samples were degassed for 12 h at 300 °C. The specific surface areas were calculated using the Brunauer–Emmett–Teller (BET) equation based on the adsorption data obtained in the pressure ($P/P_0$) range of 0.05–0.2. The pore size distributions were obtained from the entire adsorption branch based on the Barrett–Joyner–Halenda (BJH) algorithm.

The temperature programmed desorption of ammonia ($NH_3$ TPD) was measured using a BELCAT-M (BEL Japan) instrument equipped with a thermal conductivity detector (TCD). Prior to $NH_3$ adsorption, samples were heated to 500 °C under a helium flow (30 mL $min^{-1}$) to remove the species adsorbed on the sample. After cooling to 100 °C, $NH_3$ adsorption was carried out. Subsequently, the sample was again exposed to the helium flow in order to remove weakly adsorbed $NH_3$ at 100 °C. The TPD profile was obtained while heating from 100 to 650 °C with a ramp of 10 °C $min^{-1}$ under helium flow (30 mL $min^{-1}$). The TPD profile was deconvoluted under the assumption of Gaussian distribution. Transmission electron microscope (TEM) images were obtained from the Tecnai G2 F30, with an accelerating voltage of 300 kV.

### 2.4. Pyrolysis of biomass constituents using Py-GC/MS

Catalytic pyrolysis was carried out using Py-GC/MS to evaluate the relative capabilities of catalysts to upgrade bio-oil. Experiments were performed in a vertical furnace type pyrolyzer (Py-2020D, Frontier-Lab Co.). In the non-catalytic pyrolysis experiments, about 1 mg of biomass constituent only was introduced into the metal sample cup. In the catalytic pyrolysis experiments, on the other

hand, the same amount of sample was placed on the metal sample cup, over which a small amount of quartz wool was placed. About 2 mg of catalyst was then placed above the quartz wool layer. The sample layer and the catalyst layer were separated by the intermediate wool layer to prevent contact between them. Thus, in the catalytic pyrolysis experiments, a non-catalytic pyrolysis took place first, after which the gaseous product was upgraded as it flowed through the catalyst layer. The metal sample cup containing the sample and catalyst layers was inserted into a heated pyrolyzer through which the helium carrier gas flowed.

Pyrolysis was allowed to take place for 3 min at 600 °C. The product gas was analyzed using a GC (Agilent 7890A Gas Chromatography)/MS (Agilent 5975C inert Mass Spectral Detector) which was connected directly to the pyrolyzer. A microJet cryo-trap was used for the high-resolution analysis of volatile components. The product gas was rapidly cooled and concentrated using liquid nitrogen for 3 min before it passed through the column. It was then introduced into the column by thermal desorption. An ultra alloy-5 column (30 m × 0.25 mm × 0.5 mm) was used for the GC/MS. The carrier gas was introduced into the reactor with a split ratio of 50:1. The interface temperature of the GC/MS was maintained at 300 °C. The GC oven temperature was programmed to rise from 40 °C (4 min) to 320 °C (10 min) with a ramp of 5 °C $min^{-1}$, and the total analysis time was 70 min. Each peak of the mass spectra was interpreted using the NIST05 library. Additional experiments were conducted by doubling the amount of catalyst to 4 mg in order to investigate the influence of catalyst dose, with all other conditions remaining unchanged.

## 3. Results and discussion

### 3.1. Characterization of cellulose, xylan and lignin

Table S1 (Supporting information) summarizes the results of the proximate and ultimate analyses of cellulose, xylan and lignin. The contents of water, volatiles, fixed carbon, and ash generated from each feed material were cellulose, 1.1, 95.4, 2.1 and 1.4 wt%; xylan, 3.7, 77.3, 16.7 and 2.3 wt%; and lignin, 1.7, 57.3, 34.7 and 6.3 wt%, respectively. The contents of C, H and O were cellulose 42.99, 5.94 and 50.74 wt%; xylan 40.37, 5.94 and 53.69 wt%; and lignin 47.99, 4.33 and 44.45 wt%, respectively. N and S were detected only for lignin, and were determined to be 0.14 and 3.09 wt%, respectively.

Fig. S1 (Supporting information) shows the TGA/DTG analysis results for the constituents. Most decomposition reactions were shown to be completed below 600 °C. Therefore, 600 °C was determined to be an optimal catalytic pyrolysis temperature.

### 3.2. Characterization of catalysts

The crystalline structure of UMN was confirmed by the XRD pattern exhibiting Bragg diffraction peaks (Fig. 1). Over the 2$\theta$ range of 15–25°, there was no background increase in the XRD pattern attributable to the amorphous impurities. All peaks appearing in the XRD pattern were assignable to the crystalline MFI zeolite structure. The XRD pattern exhibited only ($h\,0\,l$) reflections, which is consistent with the thickness corresponding to a single unit cell dimension along the *b*-axis [36]. The high resolution TEM image shown in Fig. 2 revealed that the UMN was composed of a random assembly of zeolite nanosheets with 2.5-nm thickness. The XRD pattern of Al-SBA-15 (data not shown) was in good agreement with that reported in the literature [31].

BET area, Si/Al ratio, pore size and pore volume are summarized in Table 1. The UMN had a large specific surface area (600 $m^2\,g^{-1}$) as well as a large pore volume (0.82 $cm^3\,g^{-1}$). This is attributed to the extremely thin thickness (2.5 nm) of the nanosheet as well as the presence of mesopores between the nanosheets [33,36]. The average pore size was 6.8 nm (Fig. S2, Supporting information). The UMN sample was synthesized so as to have an Si/Al ratio of 53. The Si/Al ratio, specific surface area, pore size, and pore volume of Al-SBA-15 were 35, 500 $m^2\,g^{-1}$, 7.8 nm, and 0.74 $cm^3\,g^{-1}$, respectively.

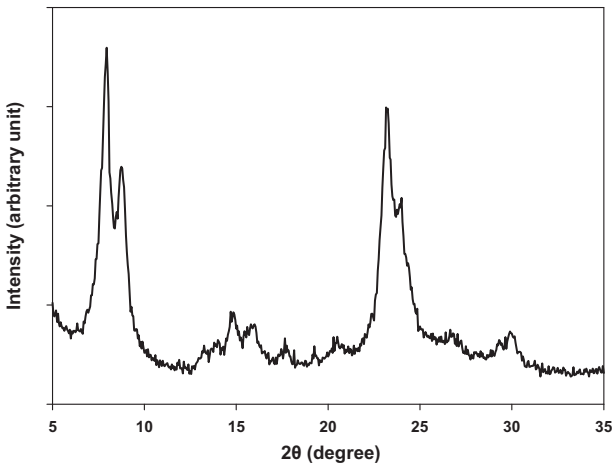


**Fig. 1.** XRD patterns of UMN.

Acid sites generated by the aluminum substitution of silicon in the crystalline framework were analyzed by $NH_3$-TPD. In the TPD profiles (Fig. 3), desorption peak appearing at the high temperature range (300–500 °C) corresponded to strong Brønsted acid sites. Al-SBA-15 was shown to have fewer acid sites with weaker strength compared to UMN.

### 3.3. Catalytic pyrolysis of biomass components

Fig. S3 (Supporting information) shows overall yields of the products of the catalytic pyrolysis of biomass components. For all the biomass components, catalytic pyrolysis increased gas yield and reduced oil yield. As pyrolytic vapors from the pyrolysis of biomass components passed through UMN catalyst, cracking and deoxygenation of pyrolytic vapors may have resulted in the reduced oil yield. Main gas components were CO, $CO_2$, and methane (Fig. S4). The increase of solid residue (char + coke) may be due to the increased coke formation.

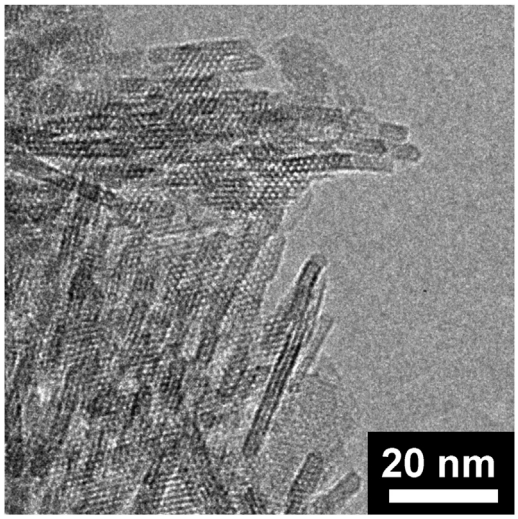


**Fig. 2.** TEM image of UMN.

**Table 1**
Physical properties of catalysts.

| Catalyst | Si/Al[a] | BET surface area ($cm^2/g$) | BJH pore size (nm) | Pore volume ($cm^3\ g^{-1}$) |
|---|---|---|---|---|
| Unilamellar MFI | 53 | 600 | 6.3 | 0.82 |
| Al-SBA-15 | 35 | 500 | 7.8 | 0.74 |

[a] Si/Al ratio from ICP/AES.

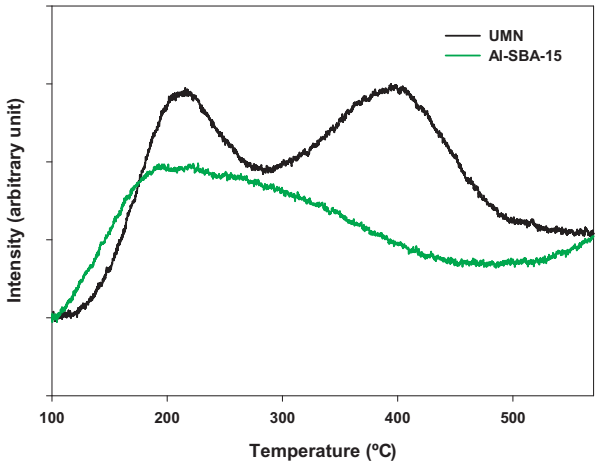


**Fig. 3.** $NH_3$ TPD of catalysts.

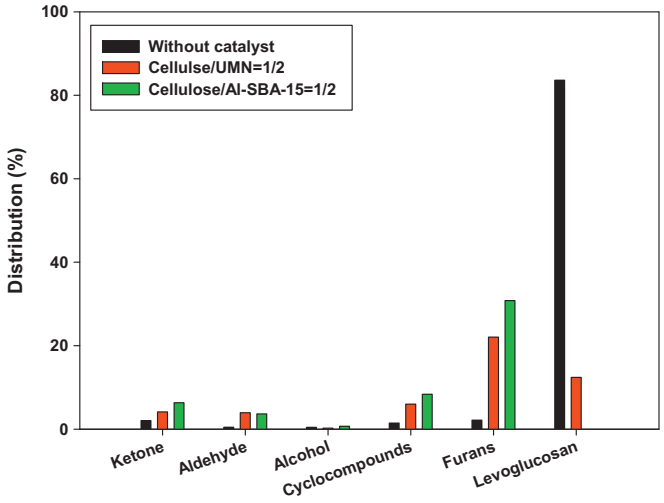


**Fig. 5.** Distribution of oxygenates from catalytic pyrolysis of cellulose.

### 3.3.1. *Catalytic pyrolysis of cellulose*

Fig. 4 shows the result of the catalytic pyrolysis of cellulose. Both Al-SBA-15 and UMN converted a considerable amount of oxygenates produced by non-catalytic pyrolysis to acids, mono-aromatics, poly aromatic hydrocarbons (PAHs), phenolics and hydrocarbons. The amounts of mono-aromatics and PAHs produced by the catalytic upgrading over the two catalysts differed to large extents, while the amounts of the other species were not very sensitive to the catalyst which was used. As shown in Fig. 5, levoglucosan accounted for the largest fraction of the product of the non-catalytic pyrolysis of cellulose. Meanwhile, for Al-SBA-15, a larger amount of furans were produced, and it is known that furans are mainly produced by the dehydration reaction of levoglucosan over acid sites [17,28,31]. However, there seems to be little further conversion of furans because Al-SBA-15 has weak acid sites. On the other hand, the upgrading over UMN resulted in a lower yield of furans and a higher yield of mono-aromatics. Furans are reportedly converted to aromatics over strong acid sites via cracking, dehydration, decarboxylation, decarbonylation and oligomerization [17,21,28,37]. Because UMN has strong Brønsted acid sites, the consecutive conversion of levoglucosan → furans → aromatics seems to be promoted. Another difference observed for the two catalysts in terms of the production of furanic compounds was the species distribution. Oxygenated furans, such as furfural and 5-methyl-2-furancarboxaldehye (5-methyl furfural), accounted for a large fraction of total furans (48.6%) when Al-SBA-15 was used, whereas the oxygen-free furan compounds, such as alkylated furan and benzofuran, accounted for a dominant fraction of total furans (77.9%) when UMN was used (Table S2, Supporting information). The strong acid sites of UMN are believed to have promoted deoxygenation reactions, such as decarbonylation and decarboxylation.

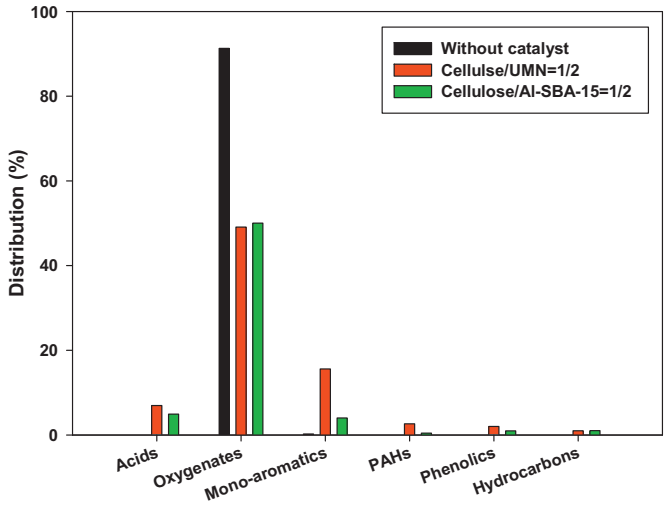


**Fig. 4.** Product distribution of catalytic pyrolysis of cellulose.

Most furans produced from catalytic pyrolysis, including furan, alkyl furans and furfural (Table S2) are important materials as organic solvents in the petrochemical industry. Therefore, the production of these compounds increases the economic value of the bio-oil. Moreover, some compounds with a high octane number, such as alkylated furan (e.g., 2,5-dimethylfuran – RON 120) can increase the energy density of a bio-oil [38]. Some compounds, such as benzofuran and ethyl-2-benzofuran, were not observed when Al-SBA-15 was used, but were produced through catalysis with UMN. This is attributed to the Diels–Alder cycloaddition reaction promoted by the Brønsted acid sites of UMN catalyzing the dehydration of furans, which is known to be the rate determining step [39,40]. Benzofuran can reportedly be further converted to aromatics [40].

Fig. S5 (Supporting information) shows the species distribution of the produced mono-aromatics. BTEX (benzene, toluene, ethylbenzene and xylene) and other aromatic compounds, such as 1,3-dimethyl-benzene, indane and indene were observed. Aromatics are important products of the pyrolysis of biomass in terms of their influence on the economic value of bio-oil, as they have high octane numbers and are used as basic feedstock materials in the petrochemical industry.

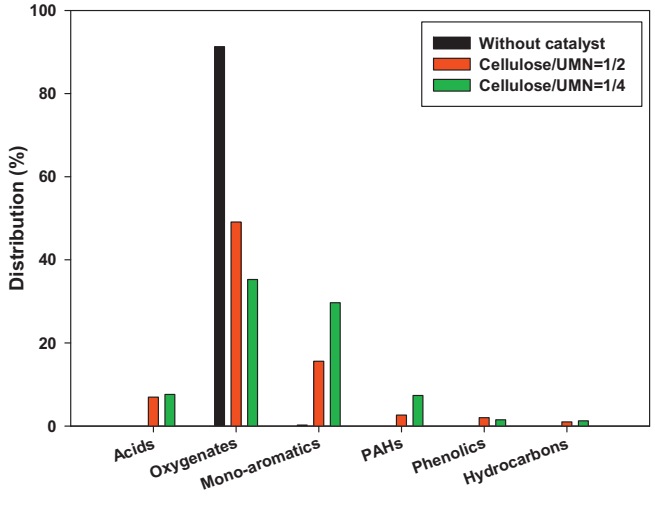


**Fig. 6.** Effect of catalyst amount on the catalytic pyrolysis of cellulose.

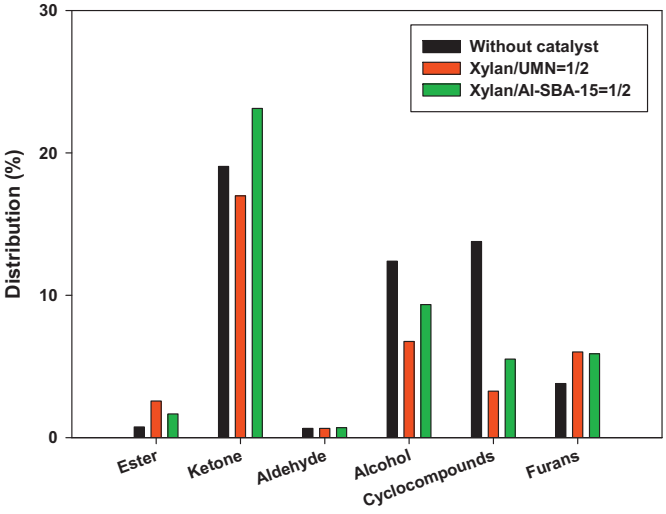


**Fig. 8.** Distribution of oxygenates from catalytic pyrolysis of xylan.

The main cyclo-compound produced over UMN was 2-cyclopenten-1-one, whereas 2-cyclopenten-1,4-dione was the main cyclo-compound produced over Al-SBA-15. It is believed that strong acid sites of UMN promoted the production of cyclo-compounds with lower oxygen contents. Naphthalene was the dominant PAH product. When separated, naphthalene can be used as raw material for the production of phthalic anhydride, naphthalene sulfonate, and naphthalene sulfonate–formaldehyde condensate [11,21].

When the cellulose/catalyst ratio was changed from 1/2 to 1/4, the content of mono-aromatics was increased considerably, from 16% to 31% (Fig. 6). The additional conversion of levoglucosan (12.4% → 2.7%), attributed to the increased quantity of acid sites, may have contributed to the increased production of aromatics. The enhanced conversion of furanic compounds to aromatics is also believed to be another reason for the enhanced production of aromatics (data not shown). The content of PAHs was also increased by increasing the catalyst dose. The yields of ketones and aldehydes were not changed significantly by increasing the catalyst dose.

### 3.3.2. *Catalytic pyrolysis of xylan*

Fig. 7 shows the product distributions obtained from the pyrolysis of xylan. Similar to the case cellulose pyrolysis, the yield of oxygenates from xylan was reduced by catalytic upgrading. The upgrading over UMN resulted in a substantial increase in the yield of mono-aromatics. In particular, the fraction of mono-aromatics was 24%, which is even larger than that obtained for cellulose (18%). Because the degree of crystallinity of hemicellulose, represented by xylan in this study, is lower than that of cellulose, it is more readily decomposed and converted into aromatics [31]. The yield of hydrocarbons was also increased slightly, contributing to an increase of the heating value of the oil. On the whole, UMN, which has stronger acidity, exhibited a better catalytic performance than Al-SBA-15; a larger amount of oxygenates was removed and the yield of aromatics was three times higher, leading to the production of a higher-quality bio-oil.

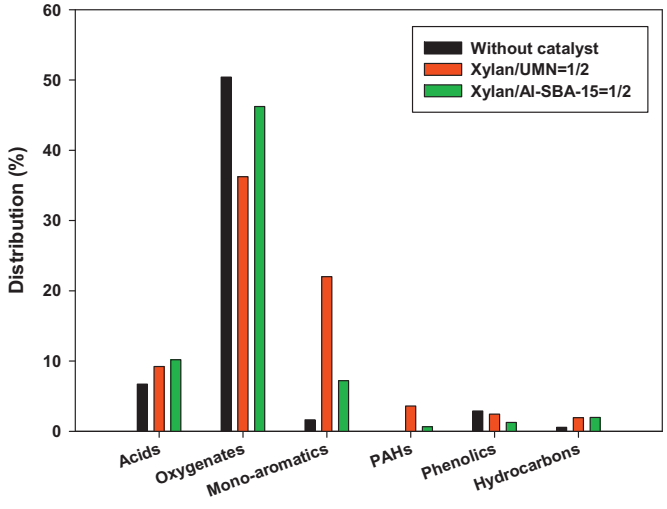


**Fig. 7.** Product distribution of catalytic pyrolysis of xylan.

When xylan was pyrolyzed in the absence of a catalyst, ketones, alcohols, and cyclo-compounds were the main oxygenate species (Fig. 8). They were converted to other species upon catalytic upgrading over UMN. In particular, alcohols (mainly ethanol) and cyclo-compounds were converted to aromatics via cracking, deoxygenation, Diels–Alder cycloaddition, and oligomerization. Ketones were also shown to undergo deoxygenation by the catalytic effect of UMN. For example, the fractions of 2-butanone and 1-hydroxy-2-butanone (4.3% and 4.5%, respectively) produced from the non-catalytic pyrolysis, were reduced considerably to 0% and 1.9%, respectively, upon catalytic upgrading over UMN. Mihalcik et al. [17] reported that ketones were converted to aromatics via decarbonylation reactions occurring on strong Brønsted acid sites when hemicellulose was pyrolyzed over HZSM-5, which is in good agreement with the results of the present study. Gayubo et al. [41] also reported that ketones were converted to aromatics in the presence of catalysts with strong acid sites, such as HZSM-5. The yield of furans, as high value-added compounds, was increased by catalytic upgrading. Mono-aromatics, which are produced from oxygenates, were mostly BTEX, 1,2,3-trimethyl-benzene, indane and 1-methyl-1H-indene (Fig. S6). Naphthalene composed the bulk of all PAHs produced.

A large quantity of acetic acid was produced from the non-catalytic pyrolysis of xylan, stemming from the decomposition of acetal groups abundant in xylan [31]. The large yield of acetic acid was not changed by catalytic upgrading. An enhanced production of acetic acids by catalytic upgrading over a mesoporous catalyst was previously reported [42]. Because acids degrade the fuel quality, causing the corrosion of engines and pipelines, appropriate treatments are required for their removal.

When the xylan/catalyst ratio was changed from 1/2 to 1/4, the fraction of aromatics increased to the largest extent (from 22% to

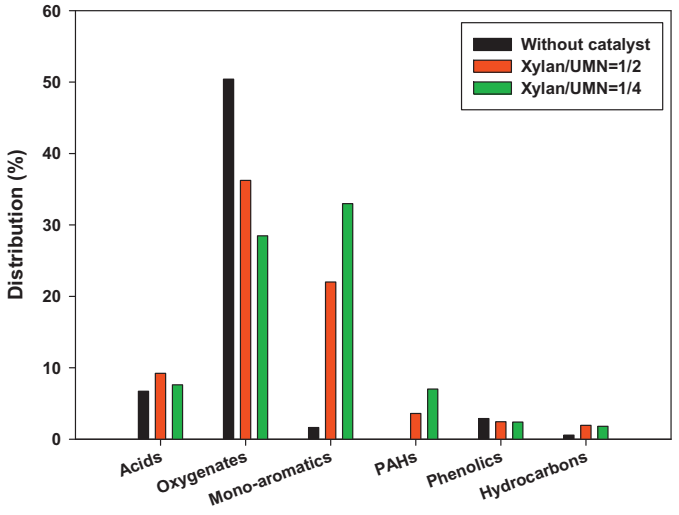


**Fig. 9.** Effect of catalyst amount on the catalytic pyrolysis of xylan.

33%) (Fig. 9). On the other hand, the fractions of oxygenate species (ketones, cyclo-compounds and furans) decreased. Like the case of cellulose, an increased catalyst dose increases the amount of acid sites that can contact with reactants, promoting cracking, decarbonylation, decarboxylation, oligomerization and aromatization, and resulting in an enhanced production of aromatics. The yield of PAHs was slightly increased, while the yield of acids was slightly decreased by catalytic upgrading.

### 3.3.3. *Catalytic pyrolysis of lignin*

Fig. 10 shows the resultant yields from the pyrolysis of lignin. Phenolics were the main products of the non-catalytic pyrolysis of lignin, as well as from pyrolysis over Al-SBA-15. However, in the case of the catalytic pyrolysis of lignin over UMN, the yield of aromatics was increased considerably.

As pointed out by Ma et al. [25], the pyrolysis of lignin produces depolymerization products via radical mechanism, which are ultimately converted to phenolics. Phenolics produced from non-catalytic pyrolysis tend to contain a large content of oxygen, having relatively high molecular masses: e.g., eugenol, 1-(4-hydroxy-3-methoxyphenyl)-ethanone, 4-(4-hydroxy-3-methoxyphenyl)-2-butanone, and 4-(ethoxymethyl)-2-methoxy-phenol). However, these species were not produced from the catalytic pyrolysis of

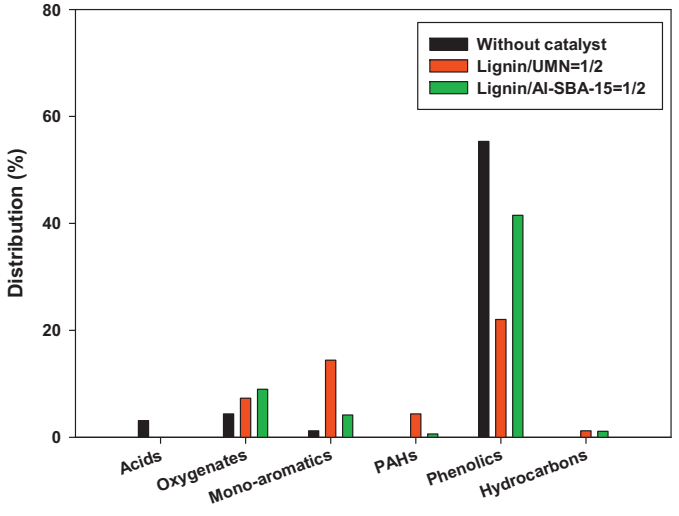


**Fig. 10.** Product distribution of catalytic pyrolysis of lignin.

lignin, and lighter phenolics with lower oxygen contents, e.g., phenol, alkyl phenols and 2-methoxy phenol were produced instead (Table 2). This can be attributed to the conversion of heavy phenolics to light phenolics via dehydration, decarbonylation, decarboxylation and cracking on the acid sites of the catalyst. Upgrading over UMN resulted in a smaller yield of methoxy phenolics than that obtained over Al-SBA-15, whereas a similar amount of alkyl phenolics were produced from catalytic pyrolysis over the two catalysts. In addition, 2-methoxy-4-(1-propenyl)-phenol and 2-methoxy-4-vinyl phenol, which are large molecules with double bonds, were removed completely by upgrading over UMN. This is attributed to the removal of methoxy groups by the demethoxylation reaction, which is promoted in the presence of the strong acid sites of UMN. Ma et al. [25] also noted that the dealkoxylation of alkoxy phenols was promoted by the strong acid sites of HZSM-5.

The yield of mono-aromatics was much higher when lignin was pyrolyzed over UMN than over Al-SBA-15 (Fig. S7, Supporting information), which was the case, too, for the pyrolysis of cellulose and xylan. Decarbonylation, decarboxylation, cracking, dealkoxylation, oligomerization and aromatization of the phenolics produced from non-catalytic pyrolysis, with the consequent production of aromatics, can occur more actively when the acidity of the catalyst is stronger. Al-SBA-15, with weaker acidity, could convert heavy phenolics to light phenolics but could not further convert light phenolics to aromatics. Ma et al. [25] also suggested that phenolics can be converted to aromatics to a sufficient extent only when sufficient acid sites are present. Park et al. [13] compared the potentials of hierarchical mesoporous MFI, Al-MCM-48 and Al-MCM-41 for the production of aromatics from the pyrolysis of miscanthus. Hierarchical mesoporous MFI, with strong acid sites, promoted the production of aromatics, whereas Al-MCM-48 and Al-MCM-41, with only weak acid sites, were adequate for the production of phenolics rather than aromatics. Thring et al. [43] carried out the catalytic pyrolysis of lignin over HZSM-5 and reported that the strong acid sites of HZSM-5 led to a high yield of aromatics. Pattiya et al. [44] also reported that in the catalytic pyrolysis of cassava rhizome, ZSM-5, with strong acid sites, produced a large quantity of aromatics, whereas mesoporous catalysts, such as Al-MCM-41, only converted large molecules to smaller molecules. The catalytic pyrolysis of spruce wood over Al-MCM-41 reduced the yield of higher-molecular-mass phenols compared to the non-catalytic pyrolysis [42]. In the catalytic pyrolysis of lignin over ZSM-5 catalysts with different Si/Al ratios [26], ZSM-5 with very weak acidity, hardly improved the quality of bio-oil, whereas ZSM-5 with strong acidity enhanced the production of light oil, while reducing heavy oil. They suggested that the strong acid sites of ZSM-5 promoted deoxygenation reactions such as decarboxylation and dehydration. These results are in good agreement with the result of the present study.

The main oxygenated species produced from the pyrolysis of lignin were furans. The yield of furans was increased by a factor of more than 2 by catalytic upgrading. Naphthalene was the main PAH species.

Doubling the catalyst dose increased the yield of mono-aromatics significantly (16% → 28%), while reducing the yield of phenolics (Fig. 11); the decrease in the fraction of methoxy phenolics was particularly large (16.2% → 2.8%). This is attributed, as mentioned above, to the promotion of reactions which convert phenolics to aromatics (decarbonylation, demethoxylation, etc.) as the number of strong acid sites is increased. Mullen and Boateng [18] reported that simple phenolics, such as phenol, are usually not converted further. In this study, however, the fraction of alkyl phenols, including phenol and methyl phenols, was decreased from 5.4% to 2.8% when the lignin/catalyst ratio was changed from 1/2 to 1/4. This indicates that the presence of a sufficient amount of

**Table 2**
Distribution of phenolics of catalytic pyrolysis of lignin.

| Phenolics | Without catalyst | Lignin/UMN = 1/2 | Lignin/UMN = 1/4 | Lignin/Al-SBA-15 = 1/2 |
|---|---|---|---|---|
| Phenol | 1.31 | 0.95 | 0.48 | 2.03 |
| 2-Methyl-phenol | 1.3 | 1.27 | 0.89 | 1.61 |
| 2,4-Dimethyl-phenol | 1.1 | 3.2 | 1.46 | 2.03 |
| 2,3,6-Trimethyl-phenol | 0 | 0 | 0 | 0.27 |
| 2-Methoxy-phenol | 17.29 | 12.6 | 2.79 | 22.75 |
| 2-Methoxy-4-methyl-phenol | 4.37 | 2.48 | 0 | 5.18 |
| 4-Ethyl-2-methoxy-phenol | 2.08 | 1.12 | 0 | 3.31 |
| 2-Methoxy-4-vinylphenol | 4.55 | 0 | 0 | 0.42 |
| 2-Methoxy-4-propyl-phenol | 0.64 | 0 | 0 | 0.6 |
| 2,6-Dimethoxy-phenol | 1.51 | 0 | 0 | 0 |
| 2-Methoxy-4-(1-propenyl)-phenol | 2.36 | 0 | 0 | 1.11 |
| 4-(Ethoxymethyl)-2-methoxy phenol | 0.92 | 0 | 0 | 0 |
| 1,2-Benzenediol | 0.58 | 0 | 0 | 0 |
| 2-Methoxy-1,4-benzenediol | 0.14 | 0 | 0 | 0 |
| Eugenol | 0.86 | 0 | 0 | 0 |
| Vanillin | 11.03 | 0 | 0 | 2.2 |
| Homovanillyl alcohol | 2.37 | 0 | 0 | 0 |
| 1-(4-Hydroxy-3-methoxyphenyl)-ethanone | 2.52 | 0 | 0 | 0 |
| 4-(4-Hydroxy-3-methoxyphenyl)-2-butanone | 0.41 | 0 | 0 | 0 |

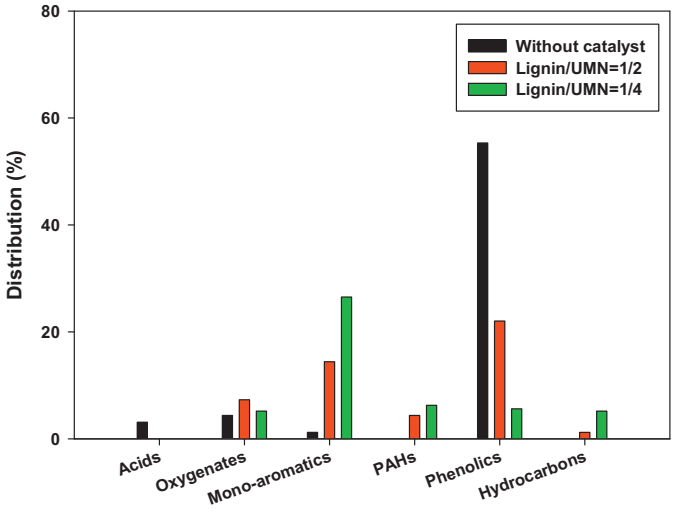


**Fig. 11.** Effect of catalyst amount on the catalytic pyrolysis of lignin.

strong acid sites enables the conversion of simple phenolics to aromatics. Ma et al. [25] also argued that an increased catalyst dose promoted the conversion of phenolics to aromatics, which is in good agreement with this study. The catalytic pyrolysis of lignin showed much higher selectivity toward high value-added BTEX than that of cellulose or hemicellulose. Further investigation of the detailed mechanisms for these pyrolysis processes is required.

The yield of oxygenates was slightly reduced by increasing the catalyst dose, whereas those of PAHs and hydrocarbons were increased. The enhanced production of hydrocarbons is beneficial in terms of oil quality because the heating value and octane number increase with increasing hydrocarbon fraction.

## 4. Conclusions

The UMN catalyst composed of a random assembly of zeolite nanosheets with a thickness of 2.5 nm exhibited superior acid characteristics, i.e., a greater number of stronger Brønsted acid sites, to the representative mesoporous catalyst Al-SBA-15. The high acidity of UMN promoted dehydration, decarboxylation, decarbonylation, cracking, oligomerization, and aromatization reactions of the bio-oil produced from the pyrolysis of biomass constituents, improving the oil quality significantly. Doubling the catalyst dose improved the oil quality even further.

UMN converted levoglucosan, the main primary oxygenate product of the pyrolysis of cellulose, to high-value-added products, such as furans and mono-aromatics. In the case of the pyrolysis of xylan, UMN converted the main non-catalytic pyrolysis products (ketones, alcohols and cyclo-compounds) to aromatics and furans. Phenolics, the main products of the non-catalytic pyrolysis of lignin, were converted by catalytic upgrading to high-value-added aromatics, including benzene, toluene, ethylbenzene and xylene and light phenolics (alkyl phenolics and methoxy phenolics). Based on the results of this study, UMN is expected to exhibit excellent catalytic activity for the catalytic pyrolysis of various lignocellulosic biomass materials.

## Acknowledgments

This research was supported by Basic Science Research Program through the National Research Foundation of Korea (NRF) funded by the Ministry of Education (2012R1A1B3003394). Also, this research was supported by the Creative Allied Project (CAP) grant funded by the Korea Research Council of Fundamental Science and Technology (KRCF)/Korea Institute of Science and Technology (KIST). In addition, R. Ryoo and W. Kim acknowledge for the support by the Institute for Basic Science in Korea.

## Appendix A. Supplementary data

Supplementary material related to this article can be found, in the online version, at http://dx.doi.org/10.1016/j.cattod.2013.12.015.

## References

[1] S.W. Kang, Y.H. Kwak, K.H. Cheon, S.H. Park, J.K. Jeon, Y.K. Park, Appl. Chem. Eng. 22 (2011) 429.
[2] I.H. Park, Y.K. Park, Y.M. Lee, W. Bae, Y.H. Kwak, K.H. Cheon, S.H. Park, Appl. Chem. Eng. 22 (2011) 286.
[3] Y.B. Jo, J.K. Jeon, S.H. Park, Y.K. Park, Appl. Chem. Eng. 23 (2012) 344.
[4] Y.B. Jo, S.H. Park, J.K. Jeon, Y.K. Park, Appl. Chem. Eng. 23 (2012) 604.
[5] W.A. Khattak, M. Ul-Islam, J.K. Park, Korean J. Chem. Eng. 29 (2012) 1467.
[6] T.A. Ngo, J.S. Kim, S.S. Kim, J. Ind. Eng. Chem. 19 (2013) 137.
[7] S.W. Kim, D.K. Park, S.D. Kim, Korean J. Chem. Eng. 30 (2013) 1162.
[8] D. Shen, R. Xiao, M. Fang, W. Chow, Korean J. Chem. Eng. 30 (2013) 228.
[9] S.J. Choi, S.H. Park, J.K. Jeon, I.G. Lee, C. Ryu, D.J. Suh, Y.K. Park, Renew. Energy 54 (2013) 105.
[10] K.H. Park, H.J. Park, J. Kim, R. Ryoo, J.K. Jeon, J. Park, Y.K. Park, J. Nanosci. Nanotechnol. 10 (2010) 355.
[11] J.W. Kim, S.H. Park, J. Jung, J.K. Jeon, C.H. Ko, K.E. Jeong, Y.K. Park, Bioresour. Technol. 136 (2013) 431.

[12] H.J. Park, H.S. Heo, J.K. Jeon, J.N. Kim, R. Ryoo, K.E. Jeong, Y.K. Park, Appl. Catal. B: Environ. 95 (2010) 365.
[13] H.J. Park, K.H. Park, J.K. Jeon, J. Kim, R. Ryoo, K.E. Jeong, S.H. Park, Y.K. Park, Fuel 97 (2012) 379.
[14] C.H. Ko, S.H. Park, J.K. Jeon, D.J. Suh, K.E. Jeong, Y.K. Park, Korean J. Chem. Eng. 29 (2012) 1657.
[15] H.J. Park, J.K. Jeon, D.J. Suh, Y.W. Suh, H.S. Heo, Y.K. Park, Catal. Surv. Asia 15 (2011) 161.
[16] H.J. Park, J.K. Jeon, S.H. Park, J.H. Yim, J.M. Sohn, Y.K. Park, J. Korean Ind. Eng. Chem. 20 (2009) 1.
[17] D.J. Mihalcik, C.A. Mullen, A.A. Boateng, J. Anal. Appl. Pyrol. 92 (2011) 224.
[18] C.A. Mullen, A.A. Boateng, Fuel Process. Technol. 91 (2010) 1446.
[19] M.A. Jackson, D.L. Compton, A.A. Boateng, J. Anal. Appl. Pyrol. 85 (2009) 226.
[20] R. French, S. Czernik, Fuel Process. Technol. 91 (2010) 25.
[21] T.R. Carlson, G.A. Tompsett, W.C. Conner, G.W. Huber, Top. Catal. 52 (2009) 241.
[22] Y. Yu, X. Li, L. Su, Y. Zhang, Y. Wang, H. Zhang, Appl. Catal. A: Gen. 447–448 (2012) 115.
[23] Y. Zhao, L. Deng, B. Liao, Y. Fu, Q.X. Guo, Energy Fuels 24 (2010) 5735.
[24] Z. Luo, S. Wang, X. Guo, J. Anal. Appl. Pyrol. 95 (2012) 112.
[25] Z. Ma, E. Troussard, J.A. van Bokhoven, Appl. Catal. A: Gen. 423–424 (2012) 130.
[26] H. Ben, A.J. Ragauskas, ACS Sustain. Chem. Eng. 6 (2013) 316.
[27] M. Käldström, N. Kumar, D. Yu Murzin, Catal. Today 167 (2011) 91.
[28] A. Aho, M. Käldström, P. Fardim, N. Kumar, K. Eränen, T. Salmi, B. Holmbon, M. Hupa, D.Y. Murzin, Cellulose Chem. Technol. 44 (2010) 89.
[29] C. Torri, I.G. Lesci, D. Fabbri, J. Anal. Appl. Pyrol. 85 (2009) 192.
[30] F.W. Yu, D.X. Ji, Y. Nie, Y. Luo, C.J. Huang, J.B. Ji, Appl. Biochem. Biotechnol. 168 (2012) 174.
[31] M.J. Jeon, J.K. Jeon, D.J. Suh, S.H. Park, Y.J.S. Sae, H. Joo, Y.K. Park, Catal. Today 204 (2013) 170.
[32] G.T. Neumann, J.C. Hicks, ACS Catal. 2 (2012) 642.
[33] M. Choi, K. Na, J. Kim, S. Yasuhiro, T. Osamu, R. Ryoo, Nature 461 (2009) 246.
[34] J. Kim, W. Park, R. Ryoo, ACS Catal. 1 (2011) 337.
[35] Y. Seo, K. Cho, Y. Jung, R. Ryoo, ACS Catal. 3 (2013) 713.
[36] K. Na, W. Park, Y. Seo, R. Ryoo, Chem. Mater. 23 (2011) 1273.
[37] M. Zabeti, T.S. Nguyen, L. Lefferts, H.J. Heeres, K. Seshan, Bioresour. Technol. 118 (2012) 374.
[38] S. Czernik, A.V. Bridgwater, Energy Fuels 18 (2004) 590.
[39] Y.T. Cheng, G.W. Huber, Green Chem. 14 (2012) 3114.
[40] Y.T. Cheng, G.W. Huber, ACS Catal. 1 (2011) 611.
[41] A.G. Gayubo, A.T. Aguayo, A. Atutxa, R. Aquado, M. Olazar, J. Bilbao, Ind. Eng. Chem. Res. 43 (2004) 2619.
[42] J. Adam, M. Blazsó, E. Mészáros, M. Stöcker, M.H. Nilsen, A. Bouzga, J.E. Hustad, M. Grønli, G. Øye, Fuel 84 (2005) 1494.
[43] R.W. Thring, S.P.R. Katikaneni, N.N. Bakhshi, Fuel Process. Technol. 62 (2000) 17.
[44] A. Pattiya, J.O. Titiloye, A.V. Bridgwater, J. Anal. Appl. Pyrol. 81 (2008) 72.